

## 823 **Supplementary Material and Methods**

824

### 825 Western blot analysis

826 Western blot analysis was done following standard procedures. Bone marrow  
827 cells were prepared using RIPA buffer or using nuclear extraction as described <sup>1</sup>. 15-  
828 25µg protein of the respective cell extracts were separated in a 5-20% gradient SDS  
829 polyacrylamid gels using electrophoresis. After transfer, nitrocellulose membranes  
830 were incubated with anti-TRF1 (Abcam, UK), anti-p53 (Santa Cruz, US), anti-SMC  
831 (Abcam, UK) or anti-Actin (Sigma, US) antibody. To detect the primary  
832 antibodybinding, a secondary antibody (Dako, Denmark) coupled to horseradish  
833 peroxidase using chemiluminescence was used (GE Healthcare, UK).

834

### 835 PCR

836 DNeasy kit (Qiagen, USA) was used for DNA isolation. PCR for genotyping of  
837 the isolated bone marrow was performed as described <sup>1</sup>. The following primer  
838 sequences were used: SA1: 5'-GCTTGCCAAATTGGGTTGG-3', E1-F2: 5'-  
839 GATGCTCGACTTCCTCT-3'.

840

### 841 RT-PCR

842 Total RNA of FACS sorted bone marrow was prepared using RNeasy Micro kit  
843 (Qiagen, USA). For first-stranded cDNA synthesis was carried out following  
844 manufacturer's instruction (Ready-to-go you-prime-first, GE Healthcare, USA).  
845 Quantitative real-time PCR was performed using DNA Master SYBR Green I mix  
846 (Applied Biosystems, US). All values were performed as duplicates and repeated at  
847 least once. The following primers were used: p21 F-:5'-GTGGGTCTGA-CTCCAGCCC-  
848 3', p21 R-:5'-CCTTCTCGTGAGACGCTTAC3'. Actin-F:5'-  
849 GGCACCACACCTTCTACAATG-3',ActinR-5'-GTGGTGGTGAAGCTGTAG-3'.

850

851 Q-FISH, immuno-Q-FISH and high throughput (HT) Q-FISH

852 Q-FISH on deparaffinized bone marrow tissue sections and image capturing  
853 were performed as described <sup>2,3</sup>. Briefly, one marrow sections were captured using a  
854 high-resolution Leica TCS-sp5 confocal microscope (Leica, US). Multi-tracking mode  
855 was used to acquire images of DAPI and Cy3 staining and stacks were taken with a  
856 step size of 0.8  $\mu\text{m}$ . Maximum projection of the images was done and Definiens XD 1.5  
857 image analysis software (Definiens GmbH, Germany) was used for quantitative image  
858 analysis. Individual telomere signals were calculated after subtraction of the mean  
859 background value per detected nucleus.

860

861 Q-FISH on bone marrow metaphases was carried out as described <sup>1,4</sup> and  
862 images were captured with 100x magnification using a Leica DMRA fluorescence  
863 microscope (Leica, US). Telomere-  $\gamma$ H2AX-immuno-Q-FISH for was performed as  
864 described<sup>1,4</sup>. Antiphospho histone H2AX (Millipore, USA) was used for  
865 immunofluorescence staining and images were captured using confocal microscope.  
866 For HT Q-FISH peripheral blood of jugular puncture was processed as described <sup>5</sup>.

867

868 Telomere length was determined analyzing telomere spots (>5000 spots) and  
869 telomere length was calculated in kilobases as described<sup>5</sup>.

870

871 Immunohistochemistry, immunofluorescence and senescence specific  $\beta$ -  
872 galactosidase staining

873 Bone marrow samples were fixed in 10% buffered formalin, decalcified,  
874 dehydrated and embedded in paraffin. For further histopathological analysis, 4  $\mu\text{m}$   
875 sections were deparaffinated and stained with hematoxylin and eosin according to  
876 standard procedures. Immunohistochemistry (IHC) of p21 (Santa Cruz Biotechnology,  
877 US), phospho-Histon3 (Millipore, US) and phospho-CHK1 (Cell Signaling Technology,  
878 US) was performed as described using the streptavidin-biotin-peroxidase method <sup>4</sup>. For

879 quantitative analysis Axio-Vision (Carl Zeiss, Germany) and Scion Image (Scion Corp.,  
880 US) software were used. Quantification of immunostaining was determined calculating  
881 the area the number of positive cells in relation to all stained nuclei.  
882 Immunofluorescence was carried out as described<sup>1,4</sup> using an anti-TRF1 antibody  
883 recently generated in our institution 6. Images were captured using confocal  
884 microscopy and image analysis was performed as described for Q-FISH. For analysis  
885 of senescence, 5-10 x10<sup>5</sup> cells were plated into 100 mm dishes and senescence  
886 specific  $\beta$ -galactosidase staining was performed following the manufacturer's  
887 instructions (Cell Signaling, US). For analysis, at least 500 cells per dish were counted.  
888  
889

890 **Supplementary References:**

- 891 1. Martinez P, Thanasoula M, Munoz P, et al. Increased telomere fragility and  
892 fusions resulting from TRF1 deficiency lead to degenerative pathologies and increased  
893 cancer in mice. *Genes Dev.* 2009;23(17):2060-2075.
- 894 2. de Jesus BB, Schneeberger K, Vera E, Tejera A, Harley CB, Blasco MA. The  
895 telomerase activator TA-65 elongates short telomeres and increases health span of  
896 adult/old mice without increasing cancer incidence. *Aging Cell*;10(4):604-621.
- 897 3. Varela E, Schneider RP, Ortega S, Blasco MA. Different telomere-length  
898 dynamics at the inner cell mass versus established embryonic stem (ES) cells. *Proc*  
899 *Natl Acad Sci U S A*;108(37):15207-15212.
- 900 4. Tejera AM, Stagno d'Alcontres M, Thanasoula M, et al. TPP1 is required for  
901 TERT recruitment, telomere elongation during nuclear reprogramming, and normal skin  
902 development in mice. *Dev Cell*;18(5):775-789.
- 903 5. Canela A, Vera E, Klatt P, Blasco MA. High-throughput telomere length  
904 quantification by FISH and its application to human population studies. *Proc Natl Acad*  
905 *Sci U S A.* 2007;104(13):5300-5305.
- 906 6. Munoz P, Blanco R, de Carcer G, et al. TRF1 controls telomere length and  
907 mitotic fidelity in epithelial homeostasis. *Mol Cell Biol.* 2009;29(6):1608-1625.
- 908
- 909

910 **Supplementary Figure Legends:**

911 Supp. Figure 1: Overview of the different injections schemata:

912 (A) Overview of the acute injection schema: Cre induction every 2nd day

913 (B) Overview of intermediate injection scheme: Daily Cre induction for 7 days

914 (C) Overview of chronic/long-term Cre induction: Cre induction 3x per week (Monday,  
915 Wednesday, Friday) up to 13 weeks

916

917 Supp. Figure 2: Immunofluorescence of TRF1<sup>flox/flox</sup>Mx1-Cre animals at day +18.

918 (A) Representative immunofluorescence of TRF1<sup>flox/flox</sup>Mx1-wt and TRF1<sup>flox/flox</sup>Mx1-Cre  
919 animals at day +18 (63x magnification and 2,5x optical zoom) (B) Quantification of  
920 TRF1 spot intensity minus background per nucleus is shown. Two-sided t-test was  
921 used for statistical comparison.

922

923 Supp. Figure 3: Intermediate 7 day Cre induction leads to a reliable and robust  
924 decrease of the bone marrow cellularity and TRF1 protein levels.

925 (A) Bone marrow cellularity calculated based on the cell number obtained from bone  
926 marrow isolation of the femura and tibiae. Two-sided t-test was used for statistical  
927 comparison.

928 (B) Western blot of TRF1 protein levels of nuclear protein extracts obtained from  
929 TRF1<sup>flox/flox</sup>Mx1-Cre animals with and without intermediate Cre induction.

930 (C) Quantification of TRF1 protein levels in relation to SMC1 levels. Two-sided t-test  
931 was used for statistical comparison.

932 (D) ELISA analysis of serum G-CSF levels of TRF1<sup>flox/flox</sup>Mx1-wt and TRF1<sup>flox/flox</sup>Mx1-  
933 Cre mice with and without intermediate Cre induction. Two-sided t-test and student t-  
934 test was used for statistical comparison.

935 (E) Cell cycle profile of TRF1<sup>flox/flox</sup>Mx1-wt and TRF1<sup>flox/flox</sup>Mx1-Cre mice with and  
936 without intermediate Cre induction. Two-sided t-test and student t-test was used for  
937 statistical comparison.

938 (F) Representative histogram of the G1, S and G2-M phase using PI staining.

939

940 Supp. Figure 4: Metaphase analysis of TRF1<sup>flox/flox</sup>Mx1-wt and TRF1<sup>flox/flox</sup>Mx1-Cre

941 mice and  $\beta$ -galactosidase staining

942 (A) Representative images of multi-telomeric signals (MTS) and chromatid fusion (CF)  
943 events (indicated by white arrow).

944 (B) Quantification of multi-telomeric signals and chromatid fusion events in  
945 TRF1<sup>flox/flox</sup>Mx1-wt and TRF1<sup>flox/flox</sup>Mx1-Cre mice undergoing intermediate Cre induction.  
946 Two-sided ttest was used for statistical comparison.

947 (C) Quantification of  $\beta$ -galactosidase staining of TRF1<sup>flox/flox</sup>Mx1-wt and TRF1<sup>flox/flox</sup>Mx1-  
948 Cre mice after 7 days of pl-pC injections and 3 days of pause before euthanizing the  
949 mice.

950

951 Supp. Figure 5: Long-term Cre induction results in compensatory higher cell

952 proliferation and replicative stress

953 (A) Representative images of phospho-histon3 IHC staining of TRF1<sup>flox/flox</sup>Mx1-wt and  
954 TRF1<sup>flox/flox</sup>Mx1-Cre mice at time point 0 and after 8 weeks of Cre induction. Image was  
955 captured with 20x magnification (blue bar represents 100  $\mu$ m), small image shows 120x  
956 magnification.

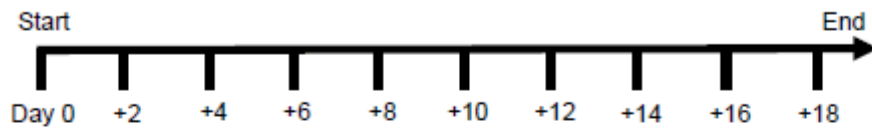
957 (B) Quantification of the phospho-histon3 IHC staining at the time points 0,+4 and +8  
958 weeks after starting Cre induction. Two-sided t-test was used for statistical comparison.

959 (C) Representative images of phospho-CHK1 IHC staining of TRF1<sup>flox/flox</sup>Mx1-wt and  
960 TRF1<sup>flox/flox</sup>Mx1-Cre mice at time point 0 and after 8 weeks of Cre induction. Image was  
961 captured with 20x magnification (blue bar represents 100  $\mu$ m), small image shows 120x  
962 magnification.

963 (D) Quantification of the phospho-CHK1 IHC staining at the time points 0,+4 and +8  
964 weeks after starting Cre induction. Two-sided t-test was used for statistical comparison.

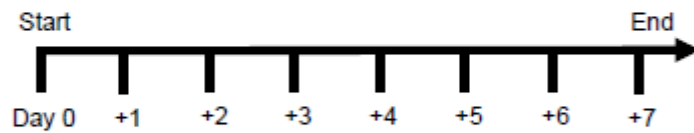
A

*Acute short-term Cre induction schema (every 2nd day)*



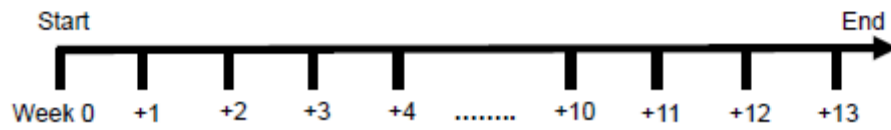
B

*Intermediate Cre induction schema (daily for 7 days)*

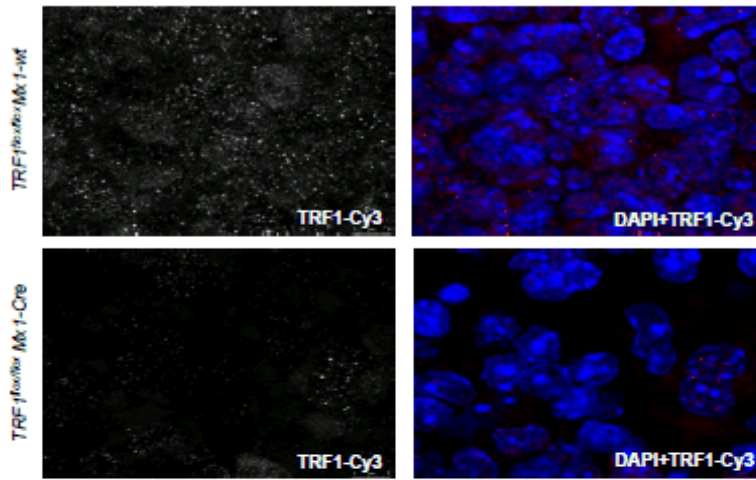


C

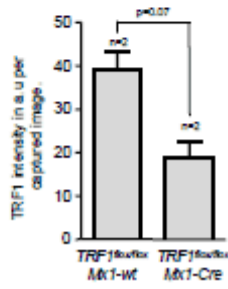
*Chronic long-term Cre induction schema (3x per week: Mo, We, Fr)*



A

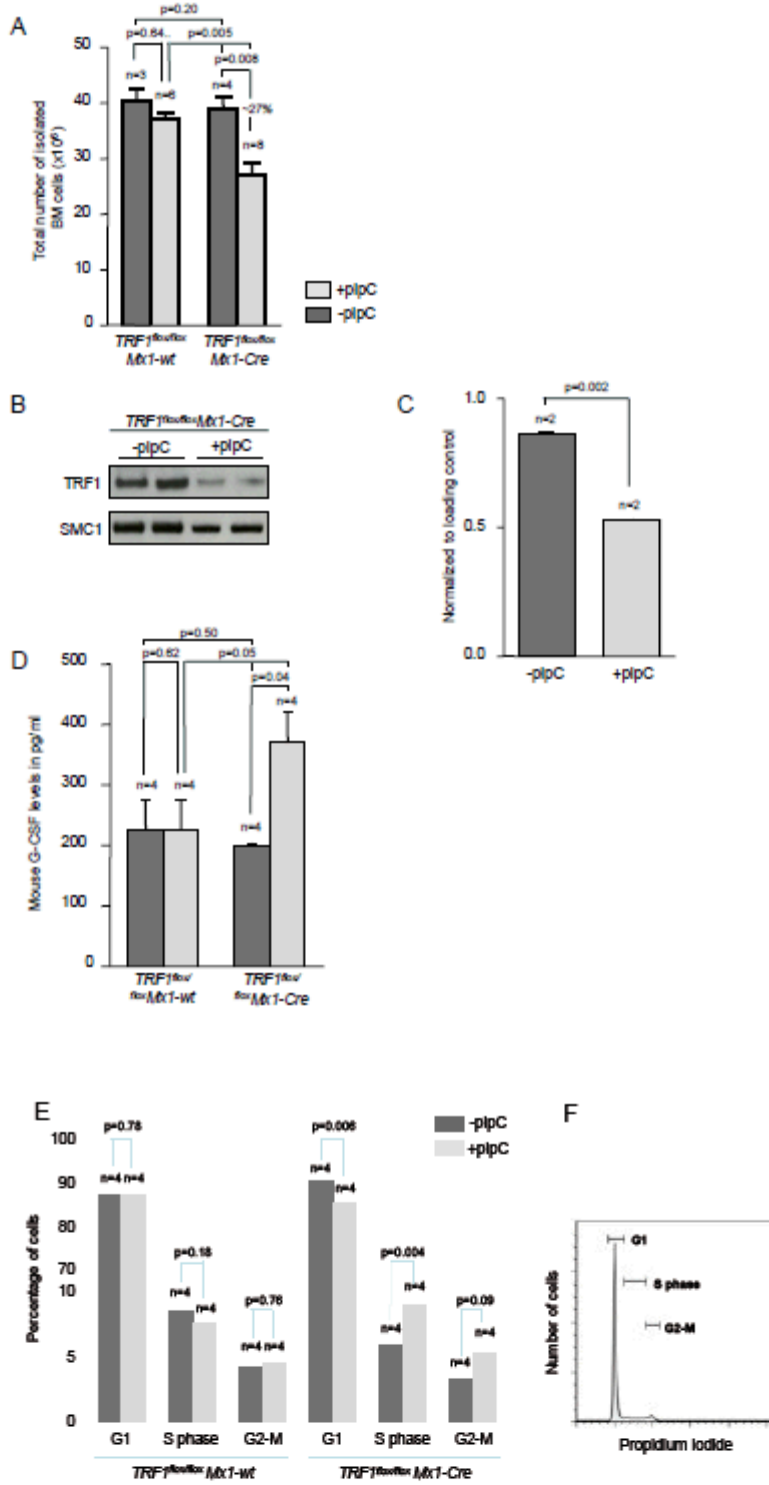


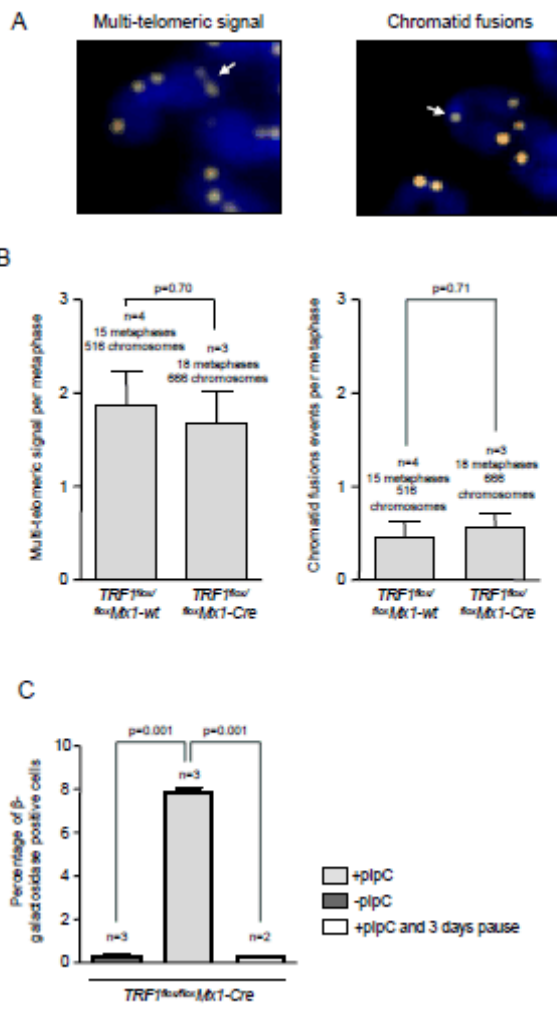
B



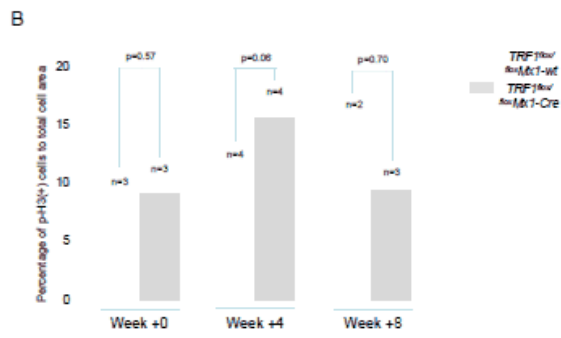
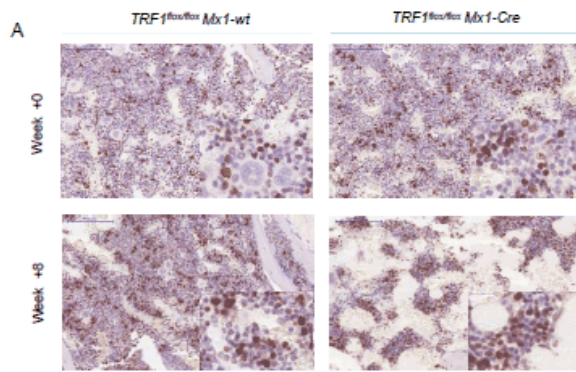
969

970

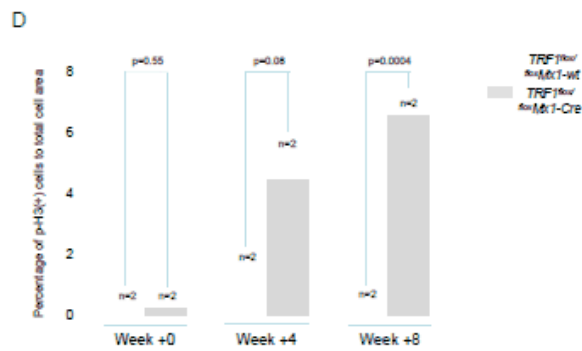
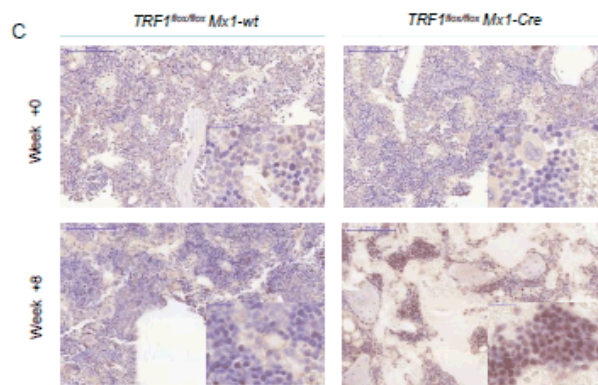




977 Supplementary Figure 5



978



979